Biosensors and Bioelectronics 54 (2014) 455–461

Contents lists available at ScienceDirect

Biosensors and Bioelectronics

journal homepage: www.elsevier.com/locate/bios

Self-powered biosensor for ascorbic acid with a Prussian blue electrochromic display

Adrianna Zloczewska [a], Anna Celebanska [a], Katarzyna Szot [a,b], Dorota Tomaszewska [a], Marcin Opallo [a], Martin Jönsson-Niedziolka [a,*]

[a] Institute of Physical Chemistry, Polish Academy of Sciences, Kasprzaka 44/52, 01-224 Warsaw, Poland
[b] Department of Molecular Biology, University of Gdansk, Wita Stwosza 59, 80-308 Gdansk, Poland

ARTICLE INFO

Article history:
Received 27 August 2013
Received in revised form
30 October 2013
Accepted 8 November 2013
Available online 21 November 2013

Keywords:
Biofuel cell
Self-powered sensor
Ascorbic acid
Prussian blue
Electrochromism
Carbon nanotubes

ABSTRACT

We report on the development of a nanocarbon based anode for sensing of ascorbic acid (AA). The oxidation of AA on this anode occurs at a quite low overpotential which enables the anode to be connected to a biocathode to form an ascorbic acid/O_2 biofuel cell that functions as a self-powered biosensor. In conjunction with a Prussian blue electrochromic display the anode can also work as a truly self-powered sensor. The oxidation of ascorbic acid at the anode leads to a reduction of the Prussian blue in the display. The reduced form of Prussian blue, called Prussian white, is transparent. The rate of change from blue to colourless is dependent on the concentration of ascorbic acid. The display can easily be regenerated by connecting it to the biocathode which returns the Prussian blue to its oxidized form. In this way we have created the first self-powered electrochromic sensor that gives quantitative information about the analyte concentration. This is demonstrated by measuring the concentration of ascorbic acid in orange juice. The reported quantitative read-out electrochromic display can serve as a template for the creation of cheap, miniturizable sensors for other relevant analytes.

1. Introduction

Interest in biofuel cells (BFCs) has mainly been focused on future application as implantable micro-power sources. Recently they gained a new role in the form of self-powered sensors (Arechederra and Minteer, 2011). The first example of such a device was described by Katz et al. (2001). The authors presented a new concept of a self-powered biosensor comprising a BFC generating different open circuit potential (OCP) dependent on the concentration of the fuel. Depending on the enzyme immobilized on the surface of the bioanode (glucose oxidase or lactate dehydrogenase) either glucose or lactate was used as a fuel/analyte. In both examples the same biocathode was used with immobilized cytochrome *c*/cytochrome oxidase responsible for dioxygen reduction. In the absence of the fuel the BFC did not generate any voltage. The OCP increased logarithmically with the increase of the fuel concentration showing the expected Nernstian dependence. Both described BFCs produced very little power to drive a device able to show the change of OCP. So the term "self-powered" was rather assigned to the fact that the cell was able to give a different output related to the change of the fuel concentration. Although in principle able to power a small read-out device, it was not demonstrated to give any signal noticeable without an externally powered device such as a potentiostat or a multimeter.

Following this definition several other self-powered biosensors were described. The Minteer group presented an example of mitochondrial bioelectrocatalysis harnessed for detecting the presence of explosives (Germain et al., 2008). As the power output was not related to the concentration of explosives, the sensor acted like a binary device detecting the presence of e.g. nitrobenzene even in 1 fM solution.

Deng et al. (2010) introduced a new approach to self-powered biosensing. They used inhibition of a BFC for sensing cyanide. In this case the decrease of the power output of a glucose/oxygen BFC was proportional to the concentration of the analyte. This effect was caused by the inhibition of laccase reducing O_2 by CN^- ions.

An interesting variant of a self-powered biosensor was developed by Hanashi et al. (2009). They used a capacitor as a transducer coupled to a light-emitting diode. The charging rate of the capacitor was proportional to the fuel concentration. When charged the capacitor was discharged through the LED, making it blink with a frequency indicative of the fuel concentration. Called the BioCapacitor the sensor was used to measure the concentration of glucose in a sample. A few more examples of devices working on the same principle were presented by Miyake et al.

* Corresponding author. Tel.: +48 22 343 3306; fax: +48 22 343 3333
E-mail address: martinj@ichf.edu.pl (M. Jönsson-Niedziolka).

0956-5663/$ - see front matter © 2013 Elsevier B.V. All rights reserved.
http://dx.doi.org/10.1016/j.bios.2013.11.033

(2011a,b) for glucose and fructose sensing. Since the readout from these type of sensors can be done with the naked eye this makes it a self-powered sensor in a more intuitive way than the Katz and Willner definition, being completely independent of external power sources.

In this paper we present a novel concept for a self-powered sensor for ascorbic acid (AA, vitamin C) based on electrochromism, i.e. the ability of some compounds to change colour when their oxidation state is changed. At the heart of the device is an AA/O_2 BFC acting as a power source. The BFC comprises an enzyme catalyzed air-breathing cathode (Zloczewska and Jönsson-Niedziolka, 2013) and a carbon based non-enzymatic anode for AA oxidation. The power output of the BFC is proportional to the concentration of AA in the electrolyte solution. Thus the BFC is in itself a self-powered sensor of the Katz-Willner type. To the best of our knowledge, this is the first example of a AA/O_2 biofuel cell demonstrated being used as a self-powered sensor. However, using the BFC to reduce or oxidize an electrochromic display we can create a reusable, truly self-powered biosensor. The device is a development of a concept presented by Möller et al. (2010) where a self-powered display was demonstrated using a viologen-based pigment. Our display is instead based on Prussian blue (PB), a dye made popular among painters in the 18th century Bartoll (2008). PB is deep blue in its oxidized state, but the reduced form is transparent. By connecting the anode of the BFC to the PB-display the dye turns transparent. The rate of the decolourization is proportional to the amount of analyte. The display can then be revived and turned into its original state by connecting it to the BFC cathode. Similarly to the BioCapacitor this kind of device is therefore a truly self-powered sensor with no external power sources needed.

A similar self-powered sensing device was very recently reported by Liu and Crooks (2012). It also contained a layer of PB which was changing the colour in the presence of the analyte, in this case glucose and hydrogen peroxide. Crooks's device has a binary function that reacts in the presence of the analyte, but gives no quantitative information. Thus, to the best of our knowledge, we present the first truly self-powered electrochromic sensor giving quantitative information of analyte concentration. We show that an AA/O_2 BFC can function as a Katz-Willner-type self-powered sensor for AA in the range from ca. 20 μM to 6 mM, covering the physiological concentrations (Procházková et al., 1998) up to those found in vitamin C rich citrus fruit (Vermeir et al., 2007). The electrochromic display is a simple, reusable sensor that can give quantitative information without any additional equipment if the display colour is compared with reference colours, like a pH strip. Used with a smart phone camera and a dedicated app, as presented by Delaney et al. (2011) for chemiluminescence, it could allow high-precision electrochromic readout of quantitative information without specialised equipment. Vitamin C is a compound essential for healthy living, and since the human body is not able to synthesize AA it needs to be provided with food. Thus a cheap sensor for AA might be a useful device. The electrochromic device was tested in the range from 1 to 6 mM AA. Its function was shown by measuring the AA-concentration in orange juice.

2. Experimental section

2.1. Materials

Pyrene-1,3,6,8-tetrasulfonic acid tetrasodium salt hydrate (PTSA), $K_3[Fe(CN)_6]$ and multiwalled carbon nanotubes (MWCNTs; OD = 20–30 nm, ID = 5–10 nm, length = 0.5–200 μm) were purchased from Sigma–Aldrich. Single walled carbon nanotubes (SWCNTs) were bought from Shenzhen Nano-tech Port Co. Ltd. Bilirubin oxidase (BOD) from Myrothecium sp. (EC 1.3.3.5) with an activity of 2.60 U/mg was donated by Amano Enzyme Inc. Toray Teflon Treated Carbon Paper TGP-H-090 was purchased from the Fuel Cell Store, CO. Methyltrimethoxysilane (MTMOS) and N-trimethoxysilylpropyl-N,N, N-trimethylammonium chloride, 50% in methanol (TMASiCl) were from ABCR and hexadecyl-trimethyl-ammonium bromide (CTAB) and tetramethoxysilane (TMOS) from Sigma–Aldrich. Tin-doped indium oxide coated glass (ITO electrodes) was obtained from Delta Technologies, Limited, USA (resistivity 8–12 Ω per square). The epoxy was prepared from an Epoxy Embedding Medium Kit (EEMK) from Fluka. Nafion Membrane N115 was from Du Pont. McIlvaine's buffer was prepared from Na_2HPO_4 (POCH S.A.) and citric acid (Chempur). Phosphate buffer was prepared from H_3PO_4 and NaOH and was used for making the solutions used in the sensor. Methanol (MeOH) and HCl were purchased from Chempur, L(+)-ascorbic acid from Riedel-de Haël and $FeCl_3 \cdot 6H_2O$ from Alfa Aesar. Negatively charged carbon nanoparticles (CNPs, ca. 7.8 nm mean diameter, Emperor 2000) were from Cabot Corporation (Dukinfield, United Kingdom). Deionised water (> 15 MΩ cm) obtained from an ELIX system (Millipore) was used for the preparation of all solutions.

2.2. Instrumentation and electrochemical measurements

All electrochemical measurements were performed on the potentiostats Autolab or μ Autolab III (Metrohm Autolab). When a standard three-electrode cell was used, $Ag|AgCl|KCl_{3M}$ electrode and platinum wire were used as a reference (RE) and counter electrode, respectively. All measurements were performed under air.

2.3. Preparation of the biofuel cell

We prepared two sets of BFCs, both with the same air-breathing biocathode, but with different anodes. The anodes were made up of ITO-electrodes modified with carbon nanomaterials. The first type of anode was modified with vertically aligned carbon nanotubes (VACNTs) and the second type with carbon nanoparticles (CNPs). The first type was prepared by gluing the carbon nanotubes to ITO electrodes according to a previously described procedure (Zloczewska et al., 2011). Briefly, VACNTs were grown in a tube furnace by thermal CVD on Si wafers with 10 nm Al_2O_3 and 1 nm layer of Fe as catalyst (700 °C, 10 sccm. acetylene, 30 min). The as-grown forests of tubes were then transferred onto the ITO electrodes and glued with a home-made conductive adhesive prepared from the EEMK mixed with MWCNTs. The active electrode surface was masked with insulating tape before being used, with the area of the projected surface from 0.015 to 0.03 cm^2. The electrodes were stored in a dry place at room temperature when not in use. The length of the VACNT was ca. 380 μm (see Fig. S4 in supplementary materials). The VACNT forests are superhydrophobic, so to enable wetting of the forest interior by the aqueous solution we briefly immersed the samples in isopropanol and then washed them with a copious amount of water. The wetted electrodes were further stored in water. The second type of anode modified with CNPs was prepared by a layer-by-layer method of silica particles and CNPs. First silicate beads (TMA-beads) were prepared via a modified Stöber method (Lesniewski et al., 2009; Stöber et al., 1968). 105.5 μl of TMASiCl and 537 μl of TMOS were mixed with 1 ml MeOH. Then 10 ml of aqueous solution of CTAB, 3 ml $NH_{3,aq}$ and 9 ml MeOH were added and constantly stirred for the next 2 h. The obtained white precipitate was filtered, washed with EtOH and left to dry in room temperature. White powder was further refluxed for 24 h with 1 mM HCl in EtOH to remove the remains of CTAB. Then it was again filtered, washed with EtOH and water and left to dry.

Suspensions of 5 mg/ml TMA-beads and CNPs were obtained by the dispersion in MeOH and acetonitrile, respectively. The ITO

electrodes were modified by alternate immersions (5 s) into the TMA-bead and CNP suspensions. Each immersion step was followed by drying in air and immersion in clean solvent to remove loosely bonded material. The active area of the electrode was limited by the Scotch tape and the electric contact was assured by a piece of a copper tape.

As a cathode for the BFC a highly efficient air-breathing electrode was used for dioxygen reduction. BOD was immobilised in a silicate matrix on Teflon treated Toray paper that functioned both as current collection and air-permeable membrane. A detailed description of the preparation and characterisation of the biocathode was recently published (Zloczewska and Jönsson-Niedziolka, 2013). The electrode was attached to the wall of a spectroscopy cuvette with a drilled hole (radius = 2.5 mm). Thanks to that construction the biocathode was able to breathe oxygen directly from the air from one side, while the other side was exposed to the electrolyte inside the cuvette. The ascorbic acid/O_2 biofuel cell was prepared by connecting the air-breathing biocathode to either a VACNT or CNP modified anode (Fig. 1).

2.4. Electrochromic display and self-powered biosensor

The electrochromic display was prepared by electrodepositing a thin film of Prussian blue onto an ITO electrode. First the ITO electrode was cleaned in ethanol and water and annealed in a tube furnace (500 °C, 15 min). The electrode was masked with an adhesive tape to define the active electrode surface (area 0.2 cm^2). PB was electrodeposited galvanostatically on the ITO electrode from a mixture of 50 mM aqueous solutions of HCl, $K_3[Fe(CN)_6]$ and $FeCl_3 \cdot 6H_2O$ in proportions 1:2:2 (García-Jareño et al., 1998). A current of 8 μA was passed through the electrode for 240 s. After this the electrode was rinsed with water, dried and put into a three-electrode cell with 0.1 M KCl solution (in phosphate buffer, pH = 4.8) where the PB display was pretreated first by keeping it at −0.05 V versus RE for 600 s (Ping et al., 2010) and then by scanning the potential 3 times from 0.6 to −0.2 V using cyclic voltammetry (scan rate = 20 mV s^{-1}). After washing with water and drying the back of the electrode was painted with white paint.

The self-powered AA sensor was made as a two-compartment cell with a Nafion membrane placed between the compartments (Fig. 1). The AA/O_2 BFC was placed in one compartment filled with the ascorbic acid solution. For this setup we used the anode modified with CNPs. The PB-display was immersed in 0.1 M KCl and placed into the second compartment. When the display was connected to the anode, the blue colour of PB faded and the display eventually turned transparent. To regenerate the display and bring back the initial blue colour, it was connected to the biocathode. At least 20 such cycles could be performed without any loss of contrast. The speed of the PB decolourization could be easily observed with the naked eye, but for more accurate observation we were also monitoring it using a camera. A Canon EOS 5D connected to a laptop was set for taking a picture each 5 s. In each picture we recorded the active display as well as a separate PB electrode kept in air.

The second electrode served as a reference colour to compare images taken under varying light conditions.

We also constructed a functioning single compartment version of the PB-display/BFC, by attaching the Nafion membrane directly in front of the PB layer. However, due to problems with leaking where the membrane was attached to the anode support this version was not used in any measurements.

3. Results and discussion

3.1. AA oxidation on the anodes

To verify the function of the anodes toward ascorbic acid oxidation cyclic voltammetry was performed in solutions of different AA concentrations (in McIlvaine's buffer, pH = 4.8) without stirring. The VACNT anodes were immersed into a new solution and left for at least 10 min before the measurement was performed to let the solution diffuse into the CNT forest. The CVs show a well defined peak with an onset potential of ca. 0.1 V and a peak potential of ca. 0.3 V (Fig. 2). In the inset of Fig. 2 the peak height is plotted as a function of the AA concentration and shows a linear relationship up to 3 mM. The linear fit gives a slope of 0.386 A cm^{-2} M^{-1}. The same experiments performed on the CNP modified anodes show that the onset of AA oxidation has been shifted to a more negative potential. The onset is already at 25 mV (Fig. 2B). However, a plot of the peak height against the AA concentration shows that the sensitivity of the CNP anodes is (Fig. 2B inset) about half of that of the VACNT anodes (slope: 0.157 A cm^{-2} M^{-1}, $R^2 = 0.999$). The likely reason for this is that the relatively large amount of AA inside the VANCT forest which functions as a thin layer cell and allows for very efficient oxidation of the trapped AA. Although the sensitivity is higher for the VANCTs, the CNP electrodes are more reproducible, both between samples and for multiple measurements using one sample. The reasons are difficulty in controlling the height of the VACNT forest, and how much of the VACNTs are active in each run as air can be trapped in the VACNT network, and that diffusion into the interior of the forest can be slow. We estimate the relative standard deviation of the VANCT electrodes to be ca. 5% and for the CNP anodes to be about 2%.

Measurements on the VACNT anode were also performed chronoamperometrically (Fig. 2C). The potential was fixed to 0.2 V. Ascorbic acid was added sequentially to reach the desired

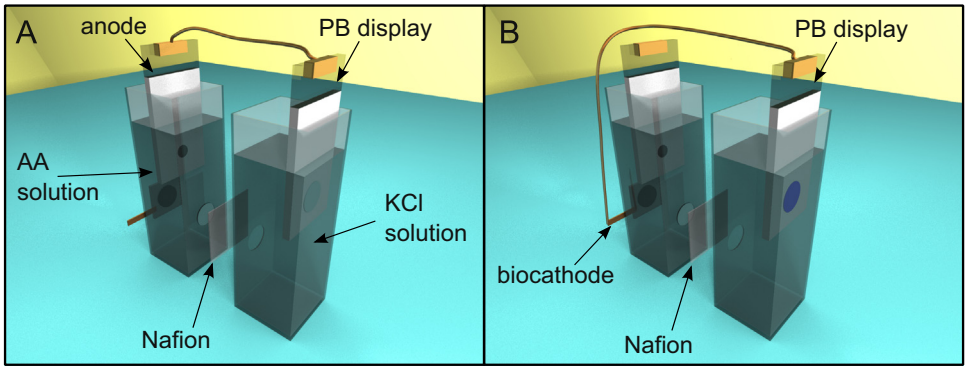

Fig. 1. A schematic illustration of the self-powered biosensor. In (A) the configuration used for AA detection and in (B) the configuration for regeneration of the PB-display. The AA/O_2 BFC is created by connecting the anode with the biocathode.

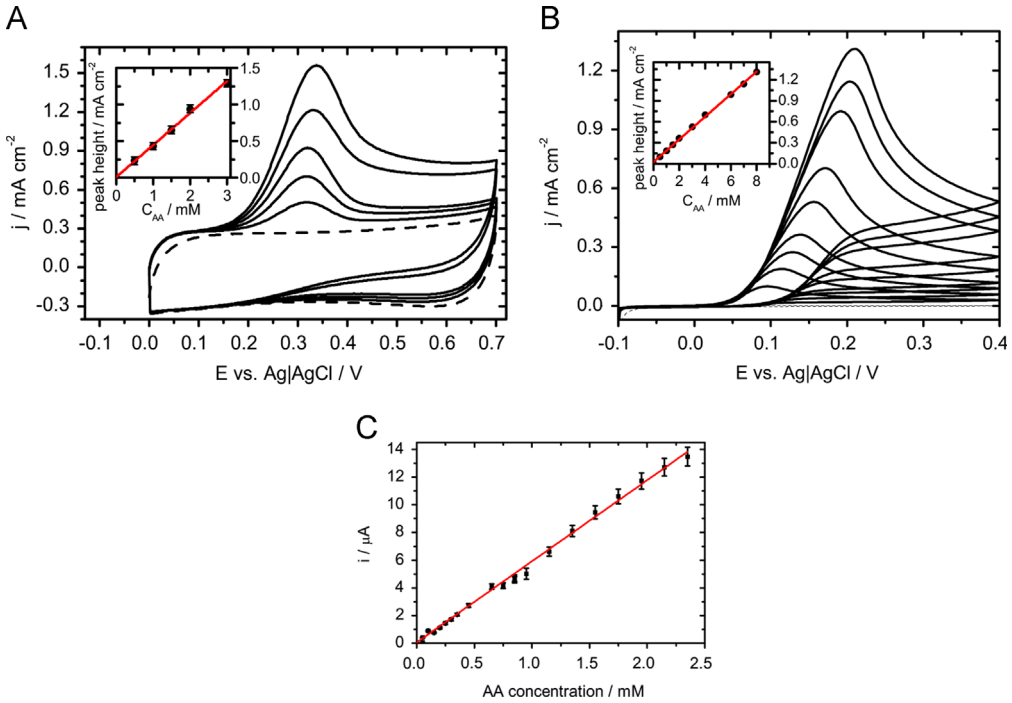

Fig. 2. (A) CV on VACNT-anode in AA solutions of different concentrations: 0 (dashed line), 0.5, 1.0, 1.5, 2.0 and 3.0 mM; $\nu = 10$ mV s^{-1}. Inset: peak height as a function of AA concentration. The line shows a least squares linear fit to the data ($R^2 = 0.998$). (B) CV on CNP film electrode in pAA solutions of different concentrations: 0.5, 1.0, 1.5, 2.0, 3.0, 4.0, 6.0, 7.0 and 8.0 mM; $\nu =$ mV s^{-1}. Inset: peak height as a function of AA concentration. The line shows a least squares linear fit to the data ($R^2 = 0.999$). (C) Current as a function of AA concentration in CA measurement using the VACNT anode. Applied potential: 0.2 V versus Ag|AgCl. The line shows a least squares linear fit to the data ($R^2 = 0.998$).

concentrations and measurements were performed after the electrolyte was thoroughly mixed for 3 min. Concentrations from 10 to 350 µM were measured. The current–concentration dependency shows a linear behaviour over the whole measurement range, and good reproducibility between different measurement runs as well as between different anodes. The calculated limit of detection is about 4 µM (at 3 times S/N). Thus the detection range of our sensors covers both the relevant levels found in human serum or urine (5.1–15.1 mg/l and 12.5–26.8 mg/l) (Procházková et al., 1998) as well as that of vitamin C rich fruits (Vermeir et al., 2007).

3.2. *AA/O_2 biofuel cells*

We used cyclic voltammetry at a slow scan rate (1 mV s^{-1}) to compare the behaviour of a separately working biocathode and VACNT-anode in 1 mM AA solution. Since the onset potential of oxygen reduction does not change significantly in the solutions of different AA concentration (data not shown) and the current of the oxygen reduction on the air-breathing electrode is at least an order of magnitude higher than the current of AA oxidation on the anode it is clear that the power of the BFC will be chiefly determined by the anode (Fig. 3A). With higher AA concentration the current generated by the BFC will grow. Experiments with the CNP modified anode showed similar result (not shown). The blue arrow in Fig. 3A indicates the difference between the onset potentials of oxygen reduction and AA oxidation. This is the open circuit potential (OCP) which can be reached by our biofuel cell. The value around 0.55 V is very similar to the OCP measured for the connected electrodes (Fig. 3C).

Polarization curves and the relationship between power and current for the VACNT biofuel cell are shown in Fig. 3C and D. These were measured with chronopotentiometry under different loadings and repeated for four different concentrations of AA: 1, 2, 4 and 6 mM. The measurements were performed under quiescent conditions and for each data point we waited for the voltage to reach a steady state after changing the load. The obtained results clearly show the dependence of the maximum power output of the BFC on the concentration of the fuel (Fig. 3B and D), which is almost linear, or, put differently, the increase of the current at a given potential. The maximum power output is reached at ca. 0.3 V independent of the AA concentration. The response to AA concentration, especially at low concentrations, is better using the CNP anode. In Fig. 3B the current at a constant potential of 0.3 V is shown using the CNP anode in AA concentrations from 50 µM to 2.25 mM. The calibration curve shows a nice linear behaviour with a sensitivity of 5.9 mA M^{-1} and a limit of determination of ca. 400 µM. As such, the AA/O_2 BFC functions as a self-powered sensor as defined by Katz et al. (2001).

The biocathode was active also in the presence of high concentration of ascorbic acid. It is known that multi-copper enzymes are quickly deactivated by ascorbic acid (Li et al., 2009). An AA/O_2 biofuel cell presented by Qian et al. (2012) was deactivated almost immediately after exposing it to 0.5 mM AA solution unless a protective ionic liquid layer was introduced to cover the cathode. They showed this effect as a very fast decrease of the OCP between the biocathode and SWCNT-anode. In 10 min the OCP dropped from 0.7 V in the buffer to almost 0 V after the addition of AA. We performed a similar experiment by measuring the OCP between the air-breathing biocathode and the VACNT anode in clean buffer solution. After 100 s the appropriate volume of concentrated AA solution was added to obtain 0.5 mM AA solution. We observed an immediate decrease of the OCP from 0.61 to 0.47 V (probably because the AA solution was added close to the cathode) but the OCP quickly recovered to 0.56 V and then gradually over several hours to 0.58 V (see Fig. 4). This robustness to AA deactivation might be explained by the repulsion of the AA anions from the negatively charged silanol groups present on the gelled matrix which acts as a protective host for BOD against AA (Lev et al., 1995).

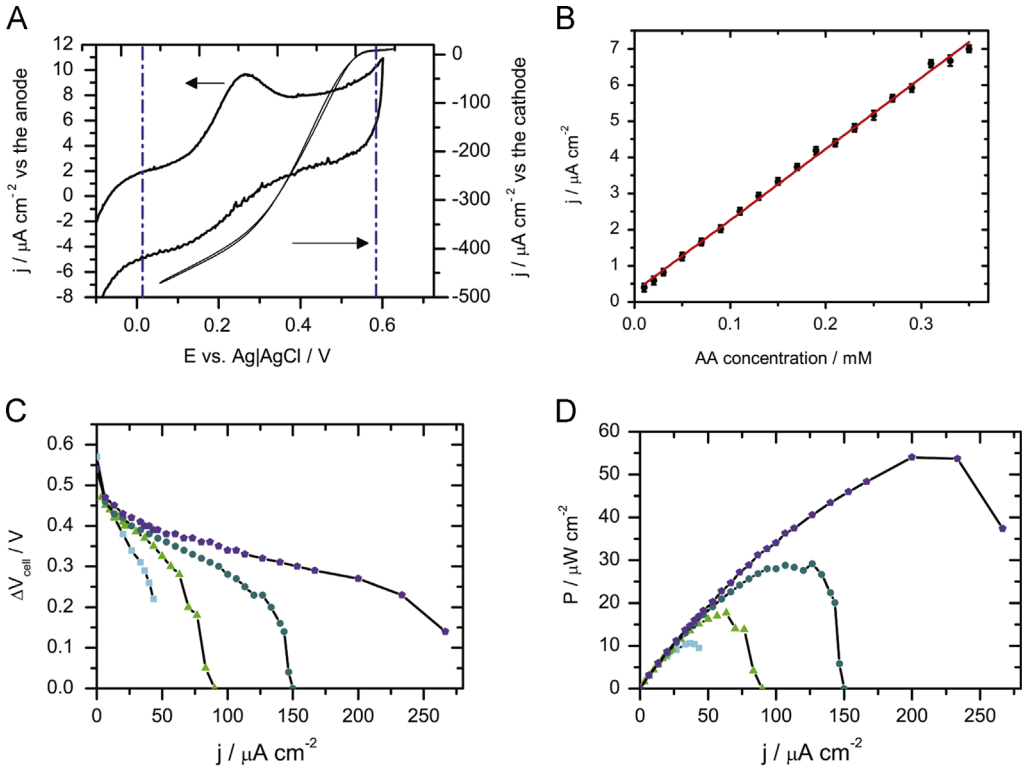

Fig. 3. (A) CV of the VACNT-anode and the biocathode working in 1 mM AA, $\nu = 1$ mV s^{-1}. The dashed blue lines indicate the onset potentials for the AA oxidation and the oxygen reduction. (B) Calibration curve for the output of the BFC with CNP anode. The current was measured at a constant potential of 0.3 V with AA concentrations from 0.05 to 2.25 mM. The line is a linear fit to the data ($R^2 = 0.97$). (C) Polarization curves (D) and the cell power as a function of current of the BFCs with VACNT anode. The measurements are shown for four different AA concentrations: 1, 2, 4 and 6 mM. (For interpretation of the references to colour in this figure caption, the reader is referred to the web version of this paper.)

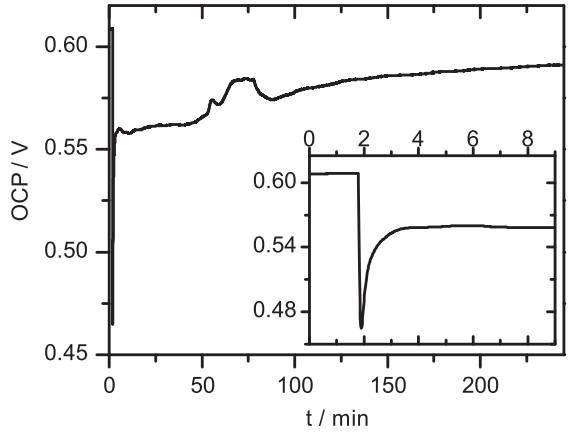

Fig. 4. Open circuit potential versus time registered for the BFC with VACNT anode. At the beginning it was measured in clean phosphate buffer (pH = 4.8). After 100 s a concentrated AA solution was added to obtain 0.5 mM solution. The inset is a zoom of the first several minutes.

3.3. Self-powered sensor for AA

The dependencies of AA concentration shown in Fig. 2 were obtained with the use of an externally powered potentiostat. Even the data from the BFC (Fig. 4) needed an external meter to be accessed. Our goal was to show these relationships in a way which used only the power generated by the BFC. To do that we picked an approach based on the use of an electrodeposited Prussian blue electrochromic display. The choice of PB for the display was made because it is an electrochromic material which starts to change its colour at a potential around 0.4 V versus Ag|AgCl|KCl_{3M}, with redox potential around 0.2 V (Itaya et al., 1982). This potential is higher than the onset potential for the AA oxidation on our anodes (ca. 0.05 V), but lower than the onset potential for O_2 reduction on our biocathode (ca. 0.6 V) (Zloczewska and Jönsson-Niedziolka, 2013). Thus, connecting the PB-display to the anode in the presence of AA will reduce the PB to its transparent form known as Everitt's salt or Prussian white. Connecting the transparent PB-display to the biocathode will return the dye to its Prussian blue form. This display reaction is likely described by the equation (Itaya et al., 1982; García-Jareño et al., 1998):

$$KFe^{III}Fe^{II}(CN)_6 + K^+ + e^- \rightleftharpoons K_2Fe^{III}Fe^{II}(CN)_6$$

and requires the presence of potassium ions. We kept our PB-display in a compartment filled with 0.1 M KCl solution. This compartment was separated from the BFC (in AA solution) via a Nafion membrane to avoid deactivation of the BOD by Cl^- ions and, more crucially, decolourization of the PB caused by its direct chemical reduction by AA (Koncki et al., 2000).

Connecting the PB-display to the CNP-anode indeed resulted in the decolourization of the electrochromic layer. The speed of the decolourization is dependent on the concentration of AA because the more AA was oxidized on the anode, the more electrons were transferred to the cathode to reduce the PB. In this experiment we used the CNP anode. The lower onset potential for AA oxidation makes it more suitable for PB reduction than the VACNT anodes. Also, the lower current compared to the VACNT anode slows down the decolourization of the PB-display which makes it easier to distinguish between different concentrations. Although one can clearly see the difference in decolourization rate with the naked eye a camera was used to take pictures of the PB-display at 5 s intervals to get an objective measure of the rate. The greyscale value (black = 0, white = 255) of the PB-display was measured automatically using ImageJ in each image and normalised with the value of a reference display. To account for differences in illumination the measured values were normalised with the value

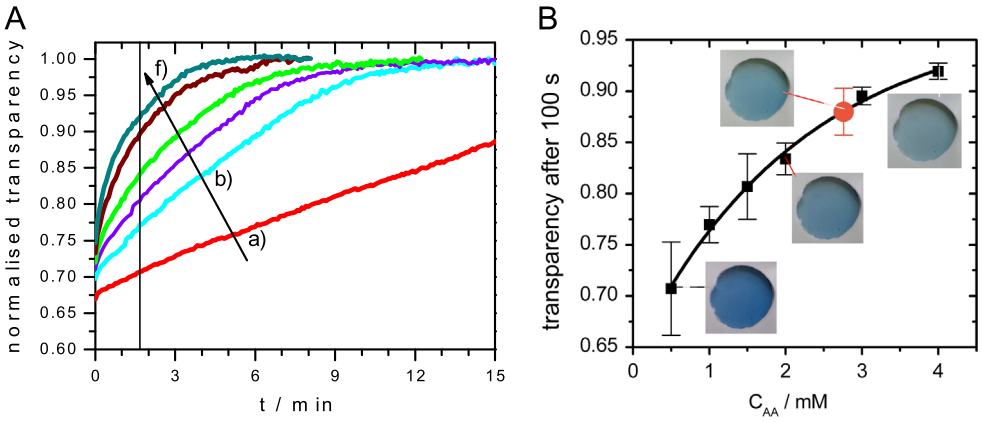

Fig. 5. (A) Normalised relative value of the change of the colour of the PB-display plotted versus time. From (a) to (f) the display was connected to the anode immersed in 0.5, 1, 1.5, 2, 3 and 4 mM AA respectively. (B) Normalised transparency of the PB-display obtained after 100 s plotted versus AA concentration. The curve is a fit to the function $y = 1 - a \times b^x$ ($R^2 = 0.993$). Photos are taken after 100 s.

of the fully reduced display. In Fig. 5A this transparency value is shown as a function of time for different concentrations of ascorbic acid. In the supplemental material a time-lapse movie shows the difference in electrode decolourization when the anode is immersed in 1 and 3 mM AA solutions. Each time after the completed fading of PB-display it was regenerated by connecting it to the biocathode of the BFC. This leads to the oxidation of the electrochromic material and the display regained its original colour in a few seconds. Due to this reversible change in the colour (see Fig. S2 in supplemental materials) a single PB-display could be used several dozen times. These results clearly show that we obtained a reusable self-powered biosensor.

A viable way of using the PB-display to determine the concentration of AA in a sample is to immerse the anode in the sample solution for a certain amount of time and then compare the colour of the display with calibration images. From Fig. 5 one can see that the largest contrast between the different samples is after about 1–2 min of exposure. After longer times the high concentration samples have already completely reduced the PB display. Fig. 5B shows the difference in colour between the different calibration samples after 100 s exposure of the anode to the AA solution. To use the sensor for checking the concentration of AA in a real sample, we filled the BFC compartment with orange juice (Tymbark). Then we took a series of pictures and analyzed them as described above. From the photo after 100 s (Fig. 5B) one can clearly see that the concentration of ascorbic acid is higher than 1 mM, and rather closer to 3 mM. For a better determination of this value we plotted the dependency of the normalized transparency obtained after 100 s versus the concentration of AA (Fig. 5B). The calibration curve asymptomatically approaches 1 as the concentration increases ($R^2 = 0.993$) and let us to find out that the concentration of AA in the juice was 2.7 ± 0.5 mM. This coincides very well with the label value of 48 mg/100 ml.

4. Conclusions

We have presented two examples of ascorbic acid/O_2 biofuel cells where both the anode and the biocathode are based on nanocarbon modified electrodes. Both cells used a highly efficient air-breathing biocathode modified with MWCNTs and bilirubin oxidase for oxygen reduction. Two different anodes were used; one based on vertically aligned carbon nanotubes and the other on layer-by-layer deposited carbon nanoparticles. The VACNT based BFC supported a higher current density than the CNP based anode, but the onset potential for AA oxidation was at more negative potential with the latter electrode. We show that the anodes themselves can work as sensitive sensors for the determination of AA concentration both voltammetrically and chronoamperometrically in a standard three-electron set-up, covering the range from physiologically relevant values in serum and urine up to the concentrations found in high vitamin C citrus fruit. Moreover, the power outputs obtained from the assembled BFCs showed close to linear dependency on the concentration of ascorbic acid. According to the definition reported by Katz et al. (2001) they can therefore be considered as self-powered biosensors.

To make a truly self-powered sensor the read-out should also be independent of external power sources. To achieve this we used a Prussian blue display as an indicator of the presence of AA at the anode. When the AA is oxidized at the anode the PB in the display is reduced and loses its blue colour and becomes transparent. By monitoring the rate of decolourization the concentration of AA in the sample can be determined. By comparing the colour of the PB-display after 100 s exposure to a sample of orange juice with calibration images we determined the AA concentration in the juice to 2.7 ± 0.5 mM, in good agreement with the value on the label. Thus our device is the first truly self-powered biosensor for ascorbic acid described so far. Moreover it presents a new approach for the construction of self-powered biosensors because by the generation of tiny currents it can act as a reversible sensor which does not use any externally powered measuring devices. Although a self-powered PB-display based sensor was recently demonstrated by Liu and Crooks (2012) this is the first example of such a device to give quantitative and not only qualitative information about the analyte concentration. We believe that electrochromic displays, possibly in combination with a mobile phone based app to monitor the colour change (Delaney et al., 2011), could be a cheap and efficient sensing option without the need for expensive apparatus. Comparison of the display colour with reference colours, like a pH strip, can make it completely independent of external apparatus. That could lead to the production of sensors utilized in everyday life by everyone who cares about his/her diet. Our AA sensor might be used for checking AA concentration in food just before the consumption, e.g. for monitoring the age of bottled orange juice (Kabasakalis et al., 2000).

Acknowledgements

The work of AZ was realized within the International PhD Projects Programme of the Foundation for Polish Science, cofinanced from the European Regional Development Fund within the Innovative Economy Operational Programme “Grants for innovation”. MJN thanks the Polish Ministry of Science and Higher Education for financing under the contract IP2011 020771. This work was supported by the

European Union within the European Regional Development Fund, through the grant Innovative Economy (POIG.01.01.02-00-008/08).

The authors thank Amano Enzyme Europe Ltd. for the donation of bilirubin oxidase; Prof. E.E.B. Campbell for the opportunity to grow the VACNTs in her lab; and Dr. W. Nogala for fruitful discussions.

Appendix A. Supplementary data

Supplementary data associated with this article can be found in the online version at http://dx.doi.org/10.1016/j.bios.2013.11.033.

References

Arechederra, R.L., Minteer, S.D., 2011. Anal. Bioanal. Chem. 400, 1605–1611.
Bartoll, J., 2008. The early use of Prussian blue in paintings. In: 9th International Conference on NDT of Art 2008, Jerusalem.
Delaney, J.L., Hogan, C.F., Tian, J., Shen, W., 2011. Anal. Chem. 83, 1300–1306.
Deng, L., Chen, C., Zhou, M., Guo, S., Wang, E., Dong, S., 2010. Anal. Chem. 82, 4283–4287.
García-Jareño, J.J., Benito, D., Navarro-Laboulais, J., Vicente, F., 1998. J. Chem. Edu. 75, 881.
Germain, M.N., Arechederra, R.L., Minteer, S.D., 2008. J. Am. Chem. Soc. 130, 15272–15273.
Hanashi, T., Yamazaki, T., Tsugawa, W., Ferri, S., Nakayama, D., Tomiyama, M., Ikebukuro, K., Sode, K., 2009. Biosens. Bioelectron. 24, 1837–1842.
Itaya, K., Ataka, T., Toshimaf, S., 1982. J. Am. Chem. Soc. 104, 4767–4772.
Kabasakalis, V., Siopidou, D., Moshatou, E., 2000. Food Chem. 70, 325–328.
Katz, E., Bückmann, A.F., Willner, I., 2001. J. Am. Chem. Soc. 123, 10752–10753.
Koncki, R., Lenarczuk, T., Glab, S., 2000. Anal. Chim. Acta 424, 27–35.
Lesniewski, A., Niedziolka-Jonsson, J., Sirieix-Plenet, J., Gaillon, L., Opallo, M., 2009. Electrochem. Commun. 11, 1305–1307.
Lev, O., Tsionsky, M., Rabinovich, L., Glezer, V., Sampath, S., Pankratov, I., Gun, J., 1995. Anal. Chem. 67, 22–30.
Li, X., Zhang, L., Su, L., Ohsaka, T., Mao, L., 2009. Fuel Cells 9, 85–91.
Liu, H., Crooks, R.M., 2012. Anal. Chem. 84, 2528–2532.
Miyake, T., Haneda, K., Nagai, N., Yatagawa, Y., Onami, H., Yoshino, S., Abe, T., Nishizawa, M., 2011a. Energy Environ. Sci. 4, 5008.
Miyake, T., Yoshino, S., Yamada, T., Hata, K., Nishizawa, M., 2011b. J. Am. Chem. Soc. 133, 5129–5134.
Möller, M., Leyland, N., Copeland, G., Cassidy, M., 2010. Eur. Phys. J. Appl. Phys. 51, 33205.
Ping, J., Mao, X., Fan, K., Li, D., Ru, S., Wu, J., Ying, Y., 2010. Ionics 16, 523–527.
Procházková, A., Kriványková, L., Boček, P., 1998. Electrophoresis 19, 300–304.
Qian, Q., Su, L., Yu, P., Cheng, H., Lin, Y., Jin, X., Mao, L., 2012. J. Phys. Chem. B 116, 5185–5191.
Stöber, W., Fink, A., Bohn, E., 1968. J. Colloid Interface Sci. 26, 62–69.
Vermeir, S., Nicolaï, B.M., Verboven, P., Van Gerwen, P., Baeten, B., Hoflack, L., Vulsteke, V., Lammertyn, J., 2007. Anal. Chem. 79, 6119–6127.
Zloczewska, A., Jönsson-Niedziolka, M., 2013. J. Power Sources 228, 104–111.
Zloczewska, A., Jönsson-Niedziolka, M., Rogalski, J., Opallo, M., 2011. Electrochim. Acta 56, 3947–3953.